

Lawrence Berkeley National Laboratory

Lawrence Berkeley National Laboratory

Title

Resist-based measurement of contrast transfer function in a 0.3-NA microfield optic

Permalink

<https://escholarship.org/uc/item/4mp4w2d5>

Authors

Cain, Jason P.
Naulleau, Patrick
Spanos, Costas J.

Publication Date

2005-01-11

Resist-based measurement of the contrast transfer function in a 0.3-NA EUV microfield optic

Jason P. Cain,^{a*} Patrick Naulleau,^b Costas J. Spanos^a

^a Department of Electrical Engineering and Computer Sciences,
University of California, Berkeley, CA 94720

^b Center for X-Ray Optics, Lawrence Berkeley National Laboratory, Berkeley, CA 94720

ABSTRACT

Although extreme ultraviolet (EUV) lithography offers the possibility of very high-resolution patterning, the projection optics must be of extremely high quality in order to meet this potential. One key metric of the projection optic quality is the contrast transfer function (CTF), which is a measure of the aerial image contrast as a function of pitch. A static microfield exposure tool based on the 0.3-NA MET optic and operating at a wavelength of 13.5 nm has been installed at the Advanced Light Source, a synchrotron facility at the Lawrence Berkeley National Laboratory. This tool provides a platform for a wide variety of research into EUV lithography. In this work we present resist-based measurements of the contrast transfer function for the MET optic. These measurements are based upon line/space patterns printed in several different EUV photoresists. The experimental results are compared with the CTF in aerial-image simulations using the aberrations measured in the projection optic using interferometry. In addition, the CTF measurements are conducted for both bright-field and dark-field mask patterns. Finally, the orientation dependence of the CTF is measured in order to evaluate the effect of non-rotationally symmetric lens aberrations. These measurements provide valuable information in interpreting the results of other experiments performed using the MET and similar systems.

Keywords: Extreme ultraviolet (EUV) lithography, aerial image contrast, contrast transfer function (CTF), micro-exposure tool (MET) optic, synchrotron

1. INTRODUCTION

The continued push toward smaller feature sizes in integrated circuits has largely been enabled by advances in optical lithography technology. However, conventional optical lithography appears to finally be reaching physical limitations that make continued improvement impractical if not impossible. A number of potential next-generation lithography (NGL) technologies are currently under development to replace optical lithography. One of these candidates is extreme ultraviolet (EUV) lithography, operating at a wavelength near 13.5 nm. While EUV lithography offers great benefits in terms of resolution, there are a number of challenges involved that must be overcome if the technology is to see production use (currently targeted for the 32 nm technology node).

In order to investigate these issues, a static micro-field exposure tool based on the Micro-Exposure Tool (MET) optic and operating at a wavelength of 13.5 nm has been installed at the Advanced Light Source, a synchrotron facility at the Lawrence Berkeley National Laboratory.¹⁻³ The MET optic is composed of two multilayer-coated reflective elements and has a numerical aperture (NA) of 0.3, comparable to the value expected for first-generation EUV production tools. The field size is 600 μm \times 200 μm at the wafer, and the tool uses a scanning illuminator to provide programmable coherence control.⁴

Extremely high optical quality is required for all lithography systems, and this is particularly true in EUV lithography as the short wavelength means that wavefront errors of even 1 nm may lead to significant degradation of the aerial image. One key characteristic of a projection optical system is its ability to transfer contrast from the object (mask) plane to the image (wafer) plane. In this paper, the contrast transfer function (CTF) for the MET optic is measured in photoresist as a means of quantifying optical performance through pitch. The measurement technique used is described in Section 2. Simulation of the CTF in order to establish expected performance is discussed in Section 3, while measured results for several different photoresists are presented in Section 4. A comparison of CTF measurements made

* Further author information: (Send correspondence to J.P.C., now with Advanced Micro Devices)
J.P.C.: E-mail: jason.cain@amd.com, Telephone: 1 (408) 749-2609

using bright field and dark field mask patterns is given in Section 5, and orientation-dependence of the CTF measurements is addressed in Section 6. Finally, conclusions are presented in Section 7.

2. MEASUREMENT OF AERIAL IMAGE CONTRAST

One important factor in determining the printing performance of a lithography tool is the aerial image contrast, defined as

$$\text{Contrast} = \frac{I_{\max} - I_{\min}}{I_{\max} + I_{\min}}, \quad (1)$$

where I_{\max} and I_{\min} are the maximum and minimum aerial image intensities, respectively (Figure 1). Typically a contrast of at least 50% is required for reliable printing performance.⁵ Aerial image contrast is a function of feature size or, equivalently, of spatial frequency. For large features, the image contrast should ideally be unity, whereas for small features beyond the resolution limit of the optical system the contrast will be zero. The details of the transition between these two extremes depend on the parameters of the optical system, including numerical aperture, wavefront quality, and illumination wavelength and partial coherence. This dependence on feature size brings about the concept of the contrast transfer function (CTF), a mapping of feature size or spatial frequency to the corresponding image contrast.

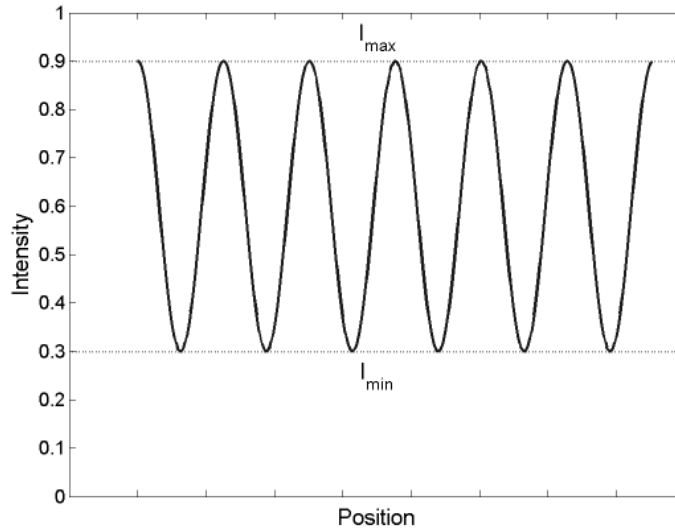


Figure 1. Illustration of factors determining aerial image contrast.

Direct measurement of aerial image contrast is challenging. In this work a photoresist threshold technique^{6,7} is applied to measure I_{\max} and I_{\min} , from which the contrast can be calculated. This process is illustrated in Figure 2. As the exposure dose is increased from Figure 2 a.)-c.), the developed linewidth shrinks (here a simple resist threshold model of development is assumed). Therefore, I_{\max} occurs at the exposure dose (D_{\max}) at which individual lines first become evident in the resist while I_{\min} occurs at the dose (D_{\min}) at which the lines vanish completely and the resist clears. Therefore, the measured contrast becomes

$$\text{Contrast} = \frac{D_{\max} - D_{\min}}{D_{\max} + D_{\min}}. \quad (2)$$

Resist images at dose levels D_{\max} and D_{\min} are shown in Figure 3. Measurement of the contrast for a range of feature sizes allows for reconstruction of the contrast transfer function.

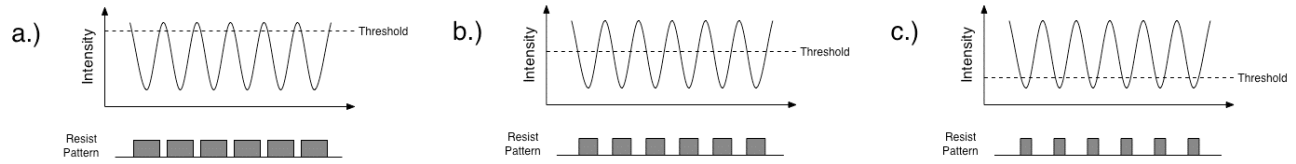


Figure 2. Principle of contrast measurement in photoresist. As the exposure dose is increased from a.) to c.), the developed linewidth shrinks.

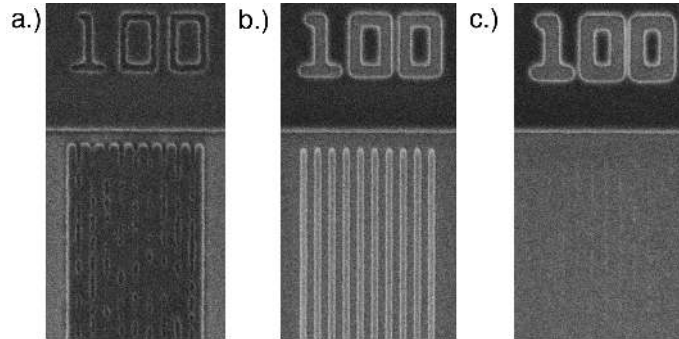


Figure 3. Post-develop resist patterns in Rohm and Haas EUV-2D resist for 100-nm features corresponding to exposure dose of a.) D_{max} , b.) mid-point between D_{max} and D_{min} , c.) D_{min} .

3. SIMULATION OF CONTRAST TRANSFER FUNCTION FOR THE MET OPTIC

The expected CTF for an optical system can be obtained through simulation given the important system parameters, including information about the wavefront quality. The expected CTF for the MET system was simulated using the PROLITH software package. In this case the lateral-shearing interferometry (LSI) measurements of the MET optic⁸ were used to accurately model the impact of aberrations on the CTF. The wavefront data for the center of the field was used, as this is where the measurements were performed. In addition, surface roughness measurements of the optical elements of the MET were used to predict the amount of flare present in the system. This predicted flare was also included in the simulations. Annular illumination was used for both simulation and experiments, with $\sigma_{inner} = 0.3$ and $\sigma_{outer} = 0.7$. The simulated CTF for vertical lines is shown in Figure 4 for both the ideal (unaberrated) and aberrated cases. The results show clearly that aberrations and flare have a strong impact on the image contrast.

4. DARK FIELD CONTRAST TRANSFER FUNCTION MEASUREMENTS

The contrast transfer function for the MET was first measured experimentally using a dark field mask, meaning that the majority of the mask area is covered with an absorber layer. Three resists were used, Rohm and Haas EUV-2D, Rohm and Haas MET-1K (XP 3454C), and a derivative of KRS.⁹ A resist thickness of 125 nm was used in each case. The PAB and PEB temperatures for EUV-2D and MET-1K were 130 °C, while KRS does not require a PEB step. Annular illumination was used, with $\sigma_{inner} = 0.3$ and $\sigma_{outer} = 0.7$. The mask pattern contained vertical lines and spaces of equal width ranging from 20 nm to 120 nm. The measurement results are shown in Figure 5.

The dark field CTF measurements show a clear dependence on the type of resist used. The apparent CTF for EUV-2D is significantly lower than for MET-1K and KRS. This is consistent with previous results, which suggest that the resolution limit for EUV-2D is higher than the limit for MET-1K. Recent results also suggest that this particular formulation of KRS has a resolution comparable to that of MET-1K.

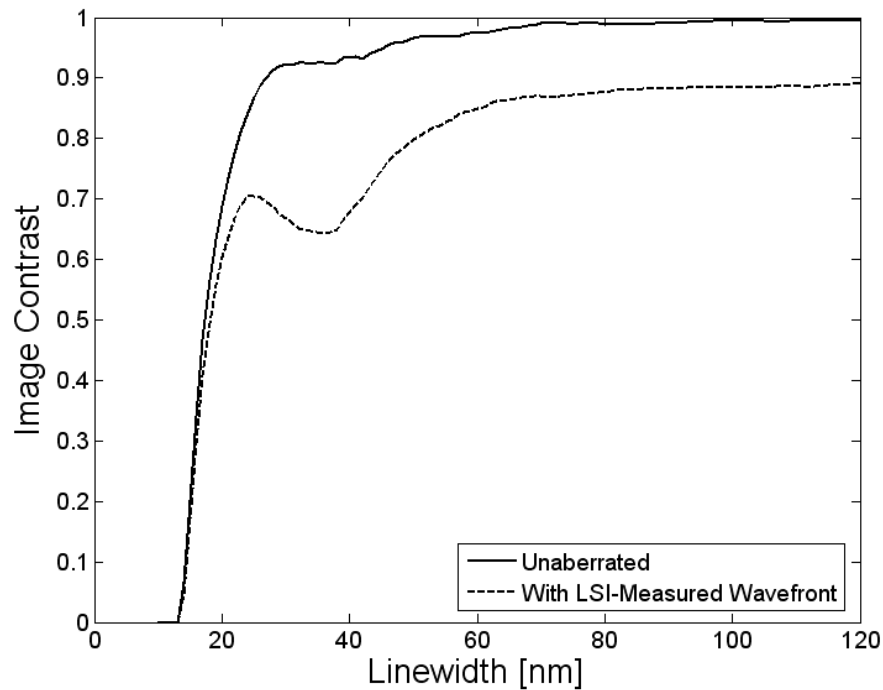


Figure 4. Simulated contrast transfer function for the MET optic under ideal, unaberrated conditions (solid line) and using the aberrated wavefront as measured using lateral shearing interferometry (dashed line).

In addition, the dark field CTF measurements show that the measured CTF is well below the value expected from simulation, even for the “high-resolution” resists. There are a number of potential sources for this difference. One possible explanation is flare. If the flare were significantly larger than predicted, this might explain at least part of the difference between measured and simulated curves. This is investigated in Section 5 by measuring the CTF for both dark field and bright field cases. A second possible explanation is aberrations. The simulation results in Figure 4 showed that aberrations have a strong effect on the CTF. Previous results⁷ have shown that the MET optic exhibits some drift in aberration level. If the aberration level has changed significantly for the worse since the interferometry experiments that provided data for the simulation were performed, this could explain the difference between simulated and measured CTF. This possibility is investigated in Section 6 by measuring the orientation-dependence of the CTF in order to detect any effects of non-rotationally symmetric aberrations. One additional explanation is simply the finite resolution of the resist due to a variety of factors such as acid diffusion length and chemical composition. This is investigated in another paper in these Proceedings.¹⁰

5. COMPARISON OF BRIGHT FIELD AND DARK FIELD CONTRAST TRANSFER FUNCTION

In order to investigate the potential effect of flare on the CTF, measurements were performed using both a bright field mask (multilayer coatings exposed over the majority of the mask area) and a dark field mask. The same resist processing and illumination parameters described in Section 4 were used in these experiments. The results for both measurements using Rohm and Haas MET-1K resist are shown in Figure 6. The error bars on the measured curves in Figure 6 represent the uncertainty due to finite exposure dose step size in the focus-exposure matrix used in the experiment.

The fact that there is no significant difference (*i.e.*, no difference outside the error bars) between the two curves indicates that flare is most likely not a dominant factor in the CTF measurements.

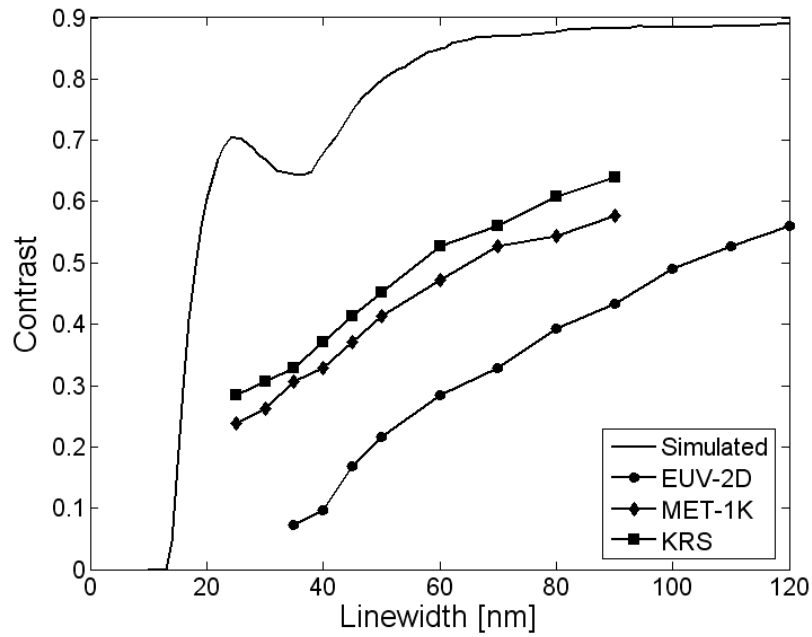


Figure 5. Contrast transfer function for the MET optic. Simulation results (including effects of aberrated wavefront) are shown along with measurements for three different resists: Rohm and Haas EUV-2D, Rohm and Haas MET-1K (XP 3454C), and a derivative of the KRS resist formulation.

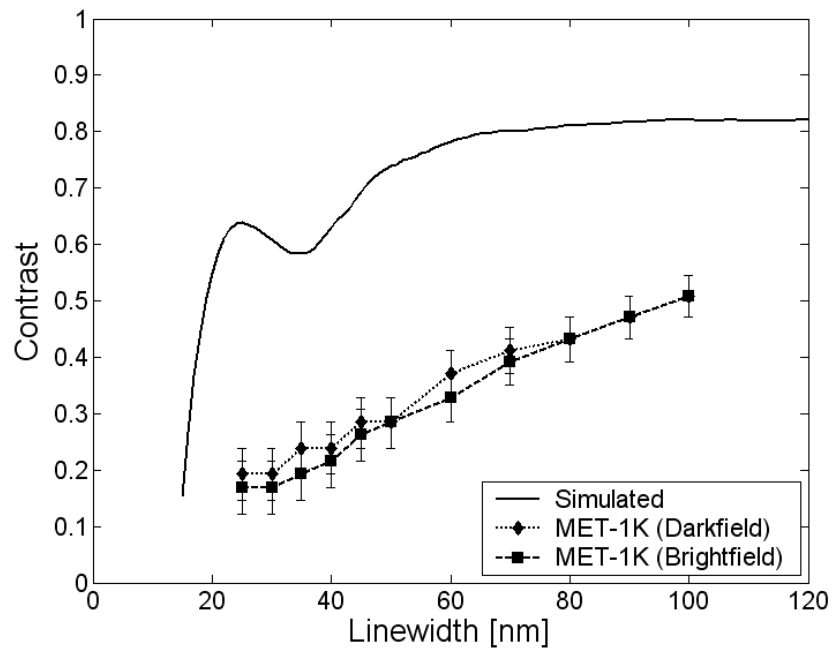


Figure 6. Comparison of dark field and bright field CTF. The error bars represent the uncertainty due to finite exposure dose step size in the focus-exposure matrix used in the experiment.

6. ORIENTATION DEPENDENCE OF CONTRAST TRANSFER FUNCTION

In order to investigate the possibility that a significant amount of aberration was introduced into the system between the interferometry measurements and the CTF measurements, the CTF was measured for four different orientations: 0° , 90° , -45° , and 45° . These measurements were conducted using elbow patterns as shown in Figure 7. If any non-rotationally symmetric aberrations are present in a significant amount, the CTF for the different orientations should show significant variation. However, it should be noted that this experiment is not able to detect the effect of rotationally symmetric aberrations such as defocus or spherical aberration.

The experiment was conducted using Rohm and Haas MET-1K (XP 3454C) resist. Annular illumination was used with $\sigma_{inner} = 0.3$ and $\sigma_{outer} = 0.7$. The results of the experiment are shown in Figure 8. The error bars in Figure 8 represent the uncertainty due to finite exposure dose step size in the focus-exposure matrix used in the experiment. The fact that there is little variation seen (no variation outside the error bars) between the CTF curves for the four orientations shown in Figure 8 is evidence that at least non-rotationally symmetric aberrations do not play a significant role in the measured CTF. This indicates that some other factors may be at work. Two of the most likely factors are resist resolution limits and spherical aberration (a rotationally symmetric aberration), which is currently being investigated.

7. CONCLUSIONS

The contrast transfer function (CTF) for the MET optic at LBNL was measured using a photoresist clearing method and compared to predicted values from simulation. These simulations included measured aberrations and flare present in the optical system. The measured CTF was significantly lower than the simulated values through pitch. In addition, a strong dependence on photoresist type was observed. The measured CTF appears to correlate with observed photoresist resolution limits. The effects of flare on the CTF were studied by measuring the CTF for both dark field and bright field mask patterns. No significant difference was observed between the two measurements, indicating that flare does not play a dominant role in determining the CTF. In addition, the effect of non-rotationally symmetric aberrations was investigated by measuring the CTF for four different feature orientations. Again, no significant differences were observed in the measurements. This indicates that non-rotationally symmetric aberrations are not present in sufficient levels to affect the CTF. However, the effect of rotationally symmetric aberrations such as spherical aberration cannot be ruled out in this experiment. Experiments are currently under way to quantify the levels of key aberrations in the MET optic (including spherical aberration) using resist-based techniques. We believe the most likely cause for the discrepancy between measured and predicted contrast to be the limited resolution of the resist.^{5,10}

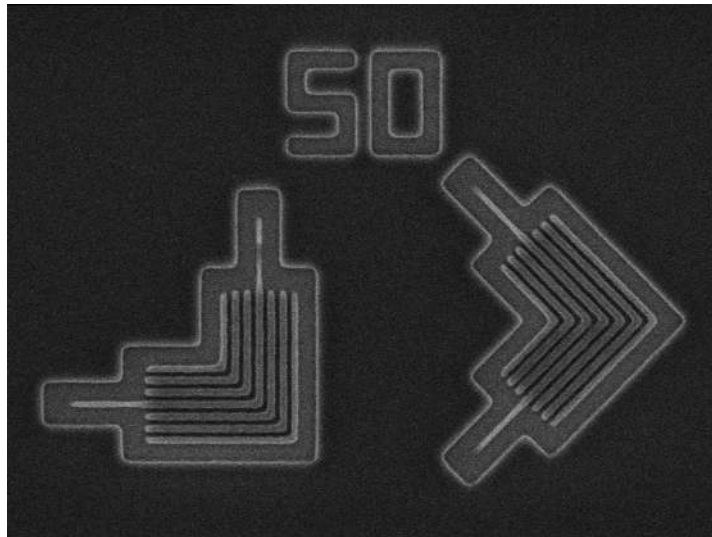


Figure 7. Example of elbow patterns used to measure orientation dependence of contrast transfer function. The nested features in this structure consist of 50 nm lines and spaces. Similar structures with line and space widths ranging from 20 nm to 100 nm were used in the measurements.

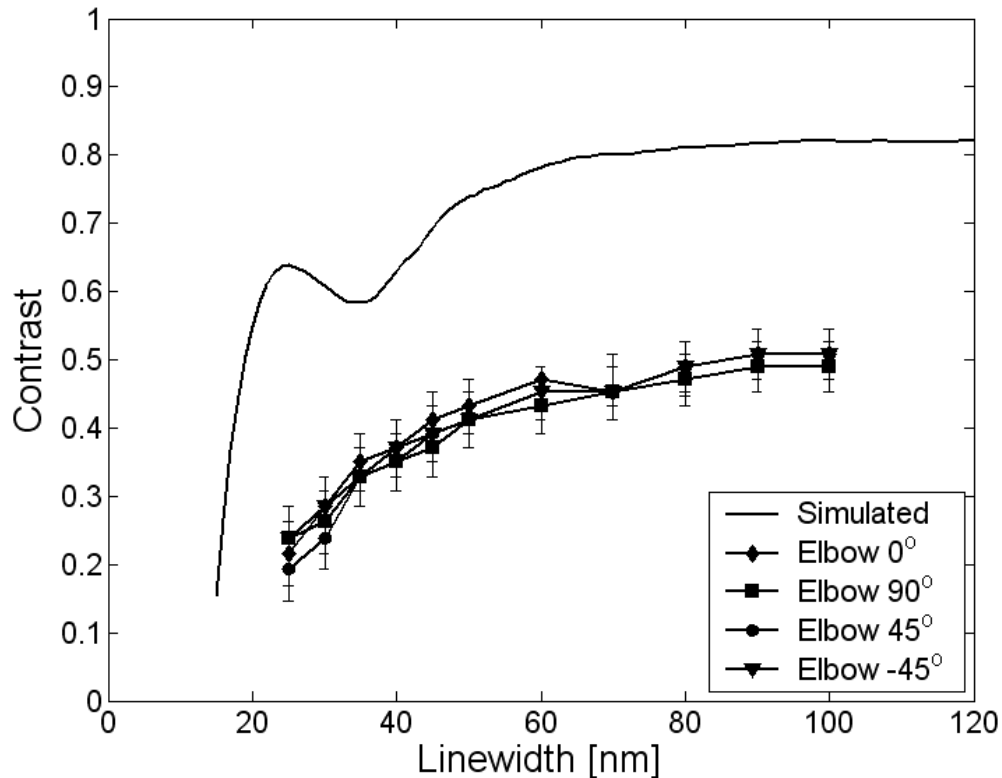


Figure 8. Contrast transfer function as measured using elbow patterns. Simulation results (including effects of aberrated wavefront) are shown along with measurements for four different orientations. The error bars represent the uncertainty due to finite exposure dose step size in the focus-exposure matrix used in the experiment.

ACKNOWLEDGMENTS

Many thanks are due to the excellent technical staff at CXRO, including Ken Goldberg, Paul Denham, Brian Hoef, and Erik Anderson. Thanks are also due to Kim Dean of SEMATECH for her support of this research, and to Robert Brainard of Rohm and Haas for resist support. Lawrence Berkeley National Laboratory is operated under the auspices of the Director, Office of Science, Office of Basic Energy Science, of the US Department of Energy. This work was funded by Advanced Micro Devices, Applied Materials, Atmel, Cadence, Canon, Cymer, DuPont, Ebara, Intel, KLA-Tencor, Mentor Graphics, Nikon Research, Novellus Systems, Panoramic Technologies, Photonics, Synopsis, Tokyo Electron, and the UC Discovery Grant.

REFERENCES

1. P. Naulleau, K. A. Goldberg, E. Anderson, K. Bradley, R. Delano, P. Denham, B. Gunion, B. Harteneck, B. Hoef, H. Huang, K. Jackson, G. Jones, D. Kemp, J. A. Liddle, R. Oort, A. Rawlins, S. Rekawa, F. Salmassi, R. Tackaberry, C. Chung, L. Hale, D. Phillion, G. Sommargren, J. Taylor, "Status of EUV microexposure capabilities at the ALS using the 0.3-NA MET optic," in *Emerging Lithographic Technologies VIII*, R. Scott Mackay, ed., Proc. SPIE **5374**, pp. 881–891, 2004.
2. P. Naulleau, K. A. Goldberg, E. Anderson, J. P. Cain, P. Denham, K. Jackson, A.-S. Morlens, S. Rekawa, F. Salmassi, "Extreme ultraviolet microexposures at the Advanced Light Source using the 0.3 numerical aperture micro-exposure tool optic," *J. Vac. Sci. Tech. B*, **22**(6), pp. 2962–2965, Nov./Dec. 2004.

3. P. P. Naulleau, K. A. Goldberg, E. H. Anderson, J. P. Cain, P. Denham, B. Hoef, K. Jackson, A. Morlens, S. Rekawa, "EUV microexposures at the ALS using the 0.3-NA MET projection optics," in *Emerging Lithographic Technologies IX*, R. Scott Mackay, ed., Proc. SPIE **5751**, 2005.
4. P. P. Naulleau, K. A. Goldberg, P. Batson, J. Bokor, P. Denham, and S. Rekawa, "Fourier-synthesis custom-coherence illuminator for extreme ultraviolet microfield lithography," *Applied Optics* **42**, pp. 820–826, February 2003.
5. S. H. Lee, D. A. Tichenor, and P. Naulleau, "Lithographic aerial-image contrast measurement in the extreme ultraviolet Engineering Test Stand," *J. Vac. Sci. Technol. B*, **20**(6), pp. 2849–2852, Nov./Dec. 2002.
6. A. Grassman and H. Moritz, "Contrast transfer function measurements of deep ultraviolet steppers," *J. Vac. Sci. Technol. B* **10**(6), pp. 3008–3011, Nov./Dec. 1992.
7. J. A. Hoffnagle, W. D. Hinsberg, M. I. Sanchez, and F. A. Houle, "Method of measuring the spatial resolution of a photoresist," *Optics Letters* **27**, pp. 1776–1778, 15 October 2002.
8. K. A. Goldberg, P. Naulleau, P. Denham, S. B. Rekawa, K. Jackson, J. A. Liddle, E. H. Anderson, "EUV interferometric testing and alignment of the 0.3 NA MET optic," in *Emerging Lithographic Technologies VIII*, R. Scott Mackay, ed., Proc. SPIE **5374**, pp. 64–73, 2004.
9. G. M. Wallraff, D. R. Medeiros, M. Sanchez, K. Petrillo, W. Huang, C. Rettner, B. Davis, C. E. Larson, L. Sundberg, P. J. Brock, W. D. Hinsberg, F. A. Houle, J. A. Hoffnagle, D. Goldfarb, K. Temple, S. Wind, and J. Bucchignano, "Sub-50 nm half-pitch imaging with a low activation energy chemically amplified photoresist," *J. Vac. Sci. Technol. B* **22**(6), pp. 3479–3484, Nov./Dec. 2004.
10. J. P. Cain, P. Naulleau, C. J. Spanos, "Modeling of EUV photoresists using resist point spread function," in *Emerging Lithographic Technologies IX*, R. Scott Mackay, ed., Proc. SPIE **5751**, 2005.